

## LARGE DEFLECTION COLLAPSE ANALYSIS OF AN INELASTIC INEXTENSIONAL RING UNDER EXTERNAL PRESSURE

S. KYRIAKIDES† and C. D. BABCOCK

California Institute of Technology, Pasadena, LA 91109, U.S.A.

(Received 9 June 1980; in revised form 18 November 1980)

**Abstract**—The problem of large deflections of an inelastic inextensional ring under external pressure is considered. The material behavior is approximated with a bilinear stress-strain curve. The nonlinear two-point boundary value problem which arises is solved numerically. It was found that the inelastic nature of the material creates a distinct limit load which represents the buckling pressure, beyond which the response path is unstable. As a result the buckling pressure of such a ring is imperfection sensitive.

### NOTATION

$E$	Young's modulus
$E'$	post yield slope of bilinear $\sigma$ - $\epsilon$ curve
$G$	normalized curvature
$H$	horizontal force at any point in ring
$\bar{H}$	$3\pi HR/\sigma_0 t^2$
$M$	moment
$M_0$	$\sigma_0 t^2/6$
$\bar{M}$	$2M/3M_0$
$P$	pressure
$P_c$	buckling pressure = $\frac{E}{4} \left( \frac{t}{R} \right)^3$
$P_0$	$\sigma_0 t/R$
$P_x$	collapse pressure
$Q$	$3\pi^2 PR/2\sigma_0 t$
$R$	ring radius
$S$	mid-plane ring coordinate
$s$	$2S/\pi R$
$t$	Ring thickness
$\underline{u}$	vector ( $\bar{H}, \bar{V}, \bar{M}, \theta$ )
$\bar{V}$	vertical force at any point on ring
$\bar{V}$	$3\pi VR/\sigma_0 t^2$
$w_0$	amplitude of initial imperfections
$x, y$	cartesian coordinates
$\bar{x}, \bar{y}$	$2(x, y)/\pi R$
$\alpha$	$E/E'$
$\Delta$	displacement of ring at $\bar{y}(1)$
$\epsilon$	strain
$\theta$	angle between normal and x-axis
$\kappa$	curvature
$\kappa_0$	curvature at first yield
$\xi$	$\sqrt{\frac{P_c}{P_0}}$
$\sigma$	stress
$\sigma_0$	yield stress

### INTRODUCTION

This paper deals with the buckling and post-buckling analysis of an inelastic ring in the large deflection regime. The small deflection initial post-buckling problem was considered by Carrier[1] (inextensional case) and by Naschie[2] (extensional case). The corresponding dynamic problem has been solved by Simmonds[3]. The question of imperfection sensitivity of the buckling pressure became a subject of controversy due to an erroneous solution by Ref. [4]. However, more careful analyses by Ref. [2, 5] have shown that the buckling pressure for the

†Presently: Department of Aerospace Engineering and Engineering Mechanics, The University of Texas, Austin, TX 78712, U.S.A.

external pressure case is insensitive to initial imperfections as shown by the positive slope of the initial post buckling curve.

Although the above arguments and analyses are correct for large diameter: thickness ratio ( $D/t > 200$ ), buckling experiments on long pipe ( $D/t < 200$ ) have repeatedly indicated contrary results. Buckling results in complete collapse of the pipe. Also imperfections, such as ovalization, have been shown to affect the value of the buckling pressure. Obviously the reason for this discrepancy is the fact that for thicker pipes or rings the material cannot be assumed elastic as in the case of the above references.

Timoshenko recognized the importance of this problem and in Ref. [6] considered the response of an elastic ring with an initial imperfection. For practical design purposes it is suggested that the critical pressure be taken to be equal to the value at which the first fiber of the ring or pipe reaches yield. The conservativeness of this statement has not been examined with a more detailed analysis.

This paper deals with the problem of collapse of a circular ring having an initial imperfection. The collapse of the ring is followed until two diametrically opposite points on the ring touch. This analysis was motivated by the relation of this problem to the problem of the so-called Propagating Buckle [7-10] where a local collapse in a long pipe under external pressure propagates flattening the whole pipe. This problem has direct implications in offshore pipelaying operations. The purpose of solving this problem was to examine the dependence of the post buckling behavior on the post yield material behavior. As a result a bilinear  $\sigma$ - $\epsilon$  curve can be accommodated. The formulation of the problem in this way leads to a system of ordinary nonlinear differential equations which are solved numerically using Newton's method.

#### THE PROBLEM

Consider a circular ring of radius  $R$  and thickness  $t$ , as shown in Fig. 1. The ring can have an initial imperfection. For convenience this will be taken to be of the form

$$w_i = w_0 \cos 2\phi \quad (1)$$

#### Equilibrium equations

The nonlinear equilibrium equations can be obtained by considering an elemental segment of the ring as shown in Fig. 2

$$\begin{aligned} \frac{dH}{dS} &= -P \cos \theta, \\ \frac{dV}{dS} &= -P \sin \theta, \end{aligned} \quad (2)$$

$$\frac{dM}{dS} = H \cos \theta + V \sin \theta.$$

$H$  and  $V$  are the horizontal and vertical forces whereas  $M$  is the moment as defined by Fig. 2.  $S$  is the coordinate along the midsurface of the ring and  $\theta$  is the angle the normal at any point makes with the  $x$ -axis.

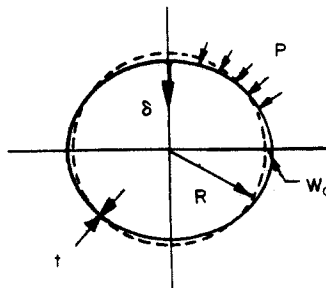


Fig. 1. Undeformed ring geometry.

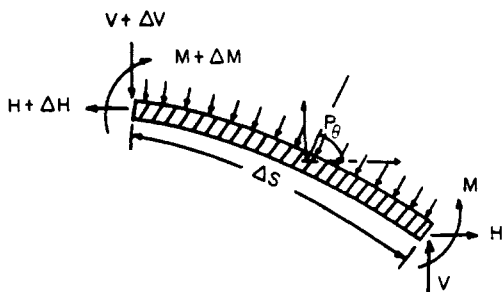


Fig. 2. Equilibrium of elemental ring section.

**Geometry**

Only the inextensional deformations of the ring will be considered, as a result

$$\frac{dx}{dS} = -\sin \theta, \tag{3}$$

$$\frac{dy}{dS} = \cos \theta,$$

where  $(x, y)$  defines a point on the deformed ring relative to the Cartesian frame shown in Fig. 1.

**Constitutive behaviour**

For the bilinear approximation of the  $\sigma$ - $\epsilon$  behavior the moment curvature relationship can be shown to be:

$$M = \frac{\sigma_0 t^2}{6} \left( \frac{\kappa}{\kappa_0} \right), \quad \text{for } M \leq \frac{\sigma_0 t^2}{6},$$

$$M = \frac{\sigma_0 t^2}{6} \left[ \frac{1}{\alpha} \left( \frac{\kappa}{\kappa_0} \right) - \frac{1}{2} \left( 1 - \frac{1}{\alpha} \right) \left( \frac{\kappa_0}{\kappa} \right)^2 + \frac{3}{2} \left( 1 - \frac{1}{\alpha} \right) \right], \quad \text{for } M > \frac{\sigma_0 t^2}{6},$$

where

$$\kappa = \frac{d\theta_0}{dS} - \frac{d\theta}{dS}; \quad \alpha = \frac{E}{E'}. \tag{4}$$

$\kappa$  is the nonlinear curvature-displacement relationship for a curved beam.  $d\theta_0/dS$  is the initial curvature.

$$\text{Let } \kappa_0 = \left\{ \kappa \mid M = \frac{\sigma_0 t^2}{6} \right\} \text{ and } G = \frac{\kappa}{\kappa_0}. \tag{5}$$

With these definitions the moment curvature relationship becomes

$$G = \bar{M}, \quad \text{for } \bar{M} \leq 1,$$

$$G^3 + \left[ \frac{3}{2}(\alpha - 1) - \alpha \bar{M} \right] G^2 - \frac{1}{2}(\alpha - 1) = 0, \quad \text{for } \bar{M} > 1, \tag{6}$$

$$\bar{M} = 6M/\sigma_0 t^2.$$

Nondimensionalizing eqns (2) and (4) appropriately, one obtains:

$$\begin{aligned}\frac{d\bar{H}}{ds} &= -Q \cos \theta, \\ \frac{d\bar{V}}{ds} &= -Q \sin \theta, \\ \frac{d\bar{M}}{ds} &= \bar{H} \cos \theta + \bar{V} \sin \theta,\end{aligned}\quad [0 \leq s \leq 1] \quad (7)$$

$$\frac{d\theta}{ds} = \frac{d\theta_0}{ds} - \pi \left(\frac{R}{t}\right) \left(\frac{\sigma_0}{E}\right) G(\alpha, \bar{M}),$$

where  $G(\alpha, \bar{M})$  is the solution of (6) with

$$\begin{aligned}G(1, \bar{M}) &= \bar{M}, \\ G(\alpha, \bar{M}) &= \bar{M} \text{ for } \bar{M} \leq 1.\end{aligned}$$

The boundary conditions are

$$\begin{aligned}\bar{H}(0) &= 0, \\ \theta(0) &= 0, \\ \theta(1) &= \pi/2, \\ \bar{V}(1) &= 0.\end{aligned}$$

In addition (3) becomes

$$\begin{aligned}\frac{d\bar{x}}{ds} &= -\sin \theta, \quad \bar{x}(1) = 0, \\ \frac{d\bar{y}}{ds} &= \cos \theta, \quad \bar{y}(0) = 0,\end{aligned}\quad [0 \leq s \leq 1] \quad (8)$$

where

$$\begin{aligned}s &= 2S/\pi R, \quad \bar{x} = 2x/\pi R, \quad \bar{y} = 2y/\pi R, \\ \bar{M} &= 6M/\sigma_0 t^2, \quad \bar{H} = 3\pi HR/\sigma_0 t^2, \quad \bar{V} = 3\pi VR/\sigma_0 t^2, \\ Q &= \frac{3}{2} \pi^2 \left(\frac{R}{t}\right)^2 \left(\frac{P}{\sigma_0}\right).\end{aligned}\quad (9)$$

(7) can be expressed in vector form as:

$$\frac{d\underline{u}}{ds} = \underline{f}(s, \underline{u}), \quad [0 \leq s \leq 1]$$

$$\underline{u} = (\bar{H}, \bar{V}, \bar{M}, \theta), \tag{10}$$

$$u_1(0) = 0, \quad u_2(1) = 0,$$

$$u_4(0) = 0, \quad u_4(1) = \pi/2.$$

Equations (10) describe a set of four nonlinear ordinary differential equations in the form of a two-point boundary value problem. Newton's iterative numerical method is used to solve for  $\underline{u}$ . The interval  $s \in [0, 1]$  is discretized into  $N$  discrete points where  $26 \leq N \leq 50$ , depending on the situation.

The convergence criterion used was as follows:

$$\max_j |u_j^{(r+1)} - u_j^{(r)}| \leq 10^{-4}.$$

The numerical method used is described in more detail in Ref. [11]. The solution of the elastic small deformation linearized problem — Ref. [6] — was used as initial guess,  $\underline{u}^{(0)}$ , to start the iteration. Then the parameter  $Q$  was increased by  $\Delta Q$  and the solution at  $Q$  was used as initial guess for  $Q + \Delta Q$ .

*Linearly elastic case ( $\alpha = 1$ )*

Linearly elastic material behavior is obtained if  $\alpha = 1$  in (7). The procedure described above is used to find the different configurations as a function of pressure (see Fig. 4). The ring was assumed to have collapsed when  $(y(1), 0) = (0, 0)$ . Figure 5 shows how the displacement (non-dimensional) of the point  $(y(1), 0)$  varies with pressure. The same study was done for five different values of the imperfection. The problem of collapse of an elastic ring with no imperfection has been studied in detail by Ref. [12], where the existence of solution is proved both above and below  $P/P_c = 1$ . In the same reference Newton's method was used to find the deformed shape as a function of pressure. For collapse as defined above,  $P/P_c = 1.68$ . This compares with a value of 1.75 found in our case. The error depends both on the mesh as well as on the convergence criterion.

More recently Sills and Budiansky[5] looked at the "initial postbuckling" of a ring with no imperfection, under external pressure. They showed that the buckling pressure is not imperfection sensitive. This was in disagreement with the results of Ref. [4]. The complete pressure-displacement curves shown in Fig. 5 clearly agree with the conclusion of Sills and Budiansky.

Pressure vs the volume change curves have also been drawn and have the same nature as those of Fig. 5; as a result they are not included.

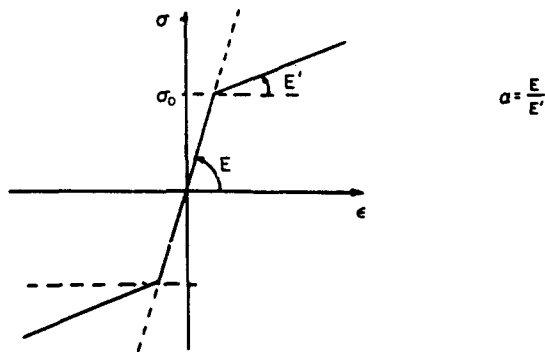


Fig. 3. Elastic-linear strain hardening material behavior assumed.

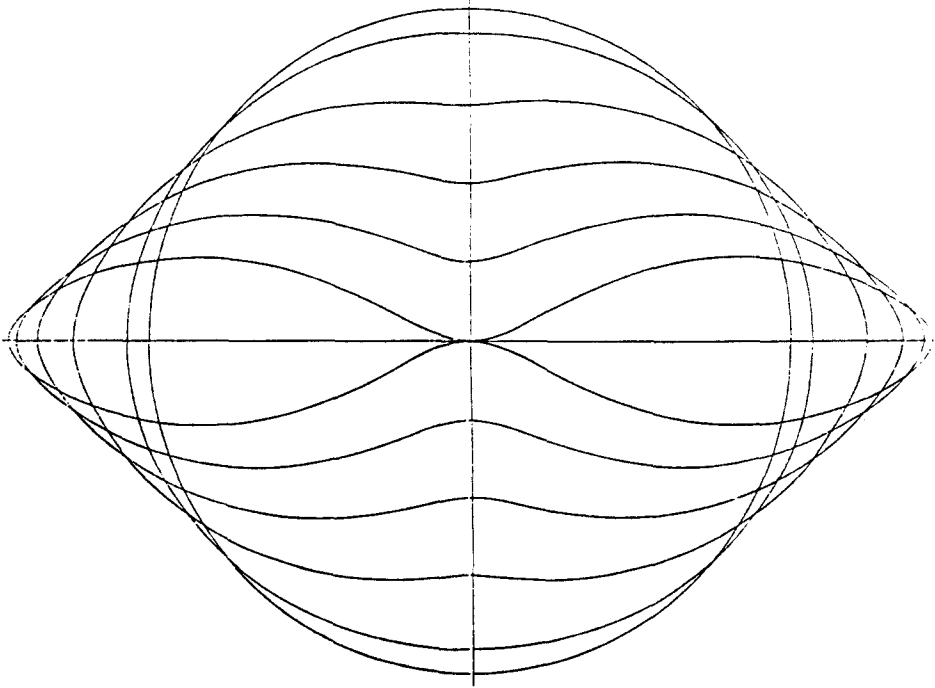


Fig. 4. Collapse sequence of a circular ring.

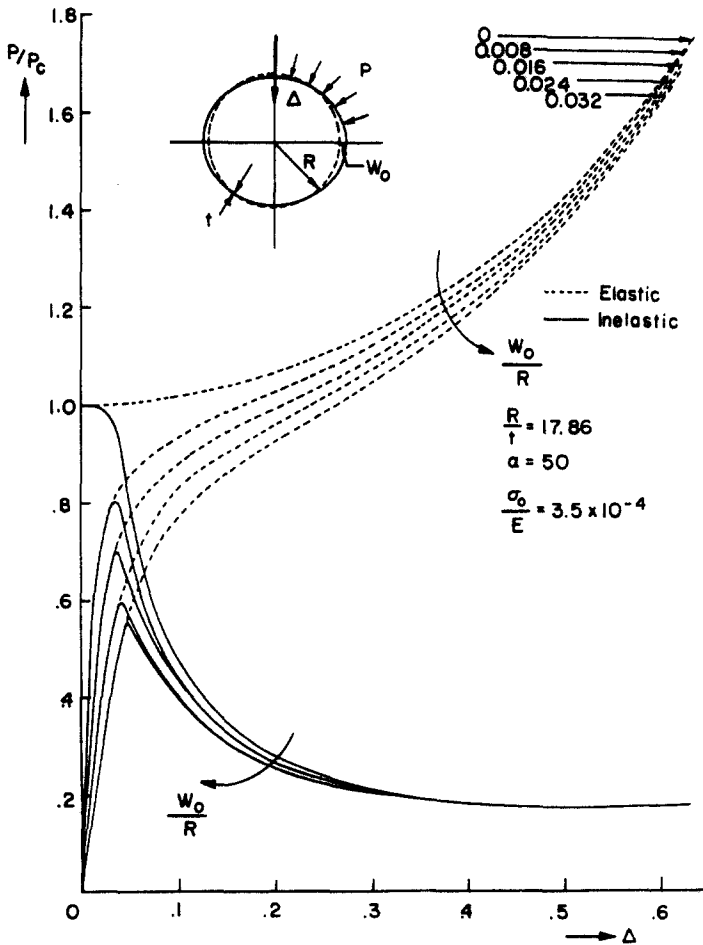


Fig. 5. Complete post buckling behavior in elastic and inelastic case.

*Linear strain hardening case* ( $\alpha > 1$ )

For many metals  $\alpha \in (50, 200)$  gives a reasonable fit to the  $\sigma$ - $\epsilon$  relation. If this range of  $\alpha$  is considered, then the pressure-displacement response changes drastically in nature. A distinct limit load appears and the ring becomes unstable beyond this point. For a pressure controlled problem (pressure increments  $\Delta Q$ ) the solution had difficulty converging for points around the limit point. Arboez in Ref. [13], facing the same problem but using the double shooting technique, successfully modified the equations so that increments of deformation were prescribed instead of load. This enabled the extension of the curve beyond the limit point. The same idea is used in this case but a different constraint is used.

From (3)

$$\frac{d\bar{y}}{ds} = \cos \theta, \quad \bar{y}(0) = 0.$$

Suppose the constraint added is:

$$\bar{y}(1) = \Delta, \text{ where } \Delta \text{ is to be prescribed each time.}$$

Since displacement cannot be prescribed simultaneously with traction at a point,  $Q$  is treated as a new unknown to the problem.

Since  $Q = \text{const}$

$$\frac{dQ}{ds} = 0.$$

Equations (7) then become

$$\frac{d\bar{H}}{ds} = -Q \cos \theta,$$

$$\frac{d\bar{V}}{ds} = -Q \sin \theta, \quad [0 \leq s \leq 1]$$

$$\frac{d\bar{M}}{ds} = \bar{H} \cos \theta + \bar{V} \sin \theta, \quad (11)$$

$$\frac{d\theta}{ds} = \frac{d\theta_0}{ds} - \pi \left( \frac{R}{t} \right) \left( \frac{\sigma_0}{E} \right) G(\alpha, \bar{M}), \quad G(1, \bar{M}) = \bar{M}$$

$$\frac{d\bar{y}}{ds} = \cos \theta, \quad G(\alpha, \bar{M}) = \bar{M} \quad \bar{M} \leq 1$$

$$\frac{dQ}{ds} = 0,$$

with B. C.'s

$$\bar{H}(0) = 0,$$

$$\theta(0) = 0,$$

$$\theta(1) = \pi/2,$$

$$\bar{V}(1) = 0,$$

$$\bar{y}(0) = 0,$$

$$\bar{y}(1) = \Delta \quad (\Delta \text{ prescribed for each calculation}).$$

In addition

$$\frac{d\bar{x}}{ds} = -\sin \theta, \quad \bar{x}(1) = 0. \tag{12}$$

The calculation now proceeded in two stages. Using increments of  $Q$  (i.e. eqns (7)), the pressure was increased to point  $k$  (see Fig. 6), a small distance below the limit point. The last converged solution (i.e. solution at point  $k$ ) was used as initial guess for the next calculation where increments of displacement  $\Delta$  were prescribed. Figure 6 shows in detail a typical example of the curve around the limit point. Increments of displacement were used until complete collapse of the ring. Figure 5 shows how the pressure displacement graphs change with the introduction of linear strain hardening. A distinct limit point is present in each case. The maximum pressure reached in each case is taken to be the buckling pressure. On collapse some residual resistance to pressure remains in the ring. The minimum pressure occurs for  $\Delta \leq 2/\pi$  (collapse condition).

Figure 7 depicts a quadrant of the ring at different stages of collapse. The spread of plasticity along the length of the ring is also shown. The region of maximum moment, (i.e. at  $s = 0$ ) goes plastic first, followed by the region at  $s = 1$ . As the deformation continues the two regions spread inwards as shown in the figure. Figure 4 shows a typical collapse sequence of a complete ring.

Figure 8 shows how the moment at  $s = 0$  (point of maximum moment for all values of  $\Delta$ ) varies with displacement. It should be noted that no unloading occurs at any value of  $\Delta$ . This is true everywhere along the ring. This fact helps simplify the numerical analysis considerably. The variation of forces at  $s = 0$  with displacement are shown in Fig. 9. Since these are the main reacting forces for the external pressure they follow the pattern of the pressure behavior with displacement  $\Delta$ .

The moment distributions around the perimeter of a ring quadrant just before buckling and on final collapse are shown in Fig. 10. Clearly the maximum moment occurs at  $s = 0$ . Similar plots for the horizontal and vertical forces are shown in Fig. 11.

RESULTS AND DISCUSSION

The same geometric parameters examined for the elastic case in Fig. 5 are examined for the inelastic case as well. The material parameters considered are  $\alpha = 50$  and  $\sigma_0/E = 3.5 \times 10^{-4}$ . The

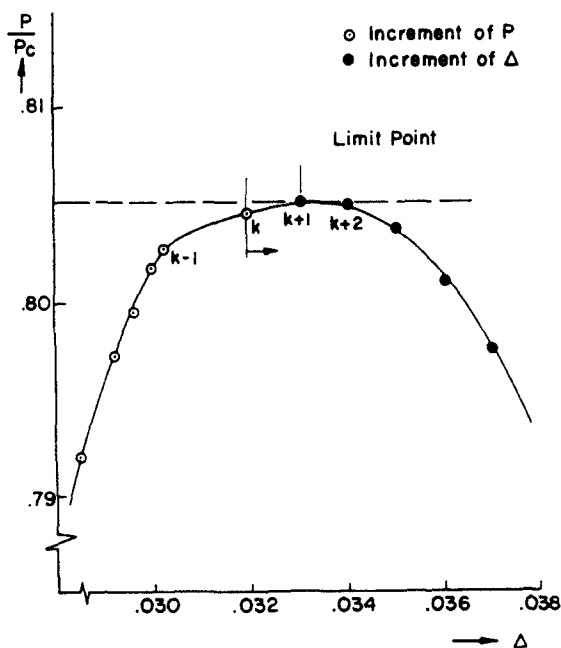


Fig. 6. Detailed drawing of limit point.



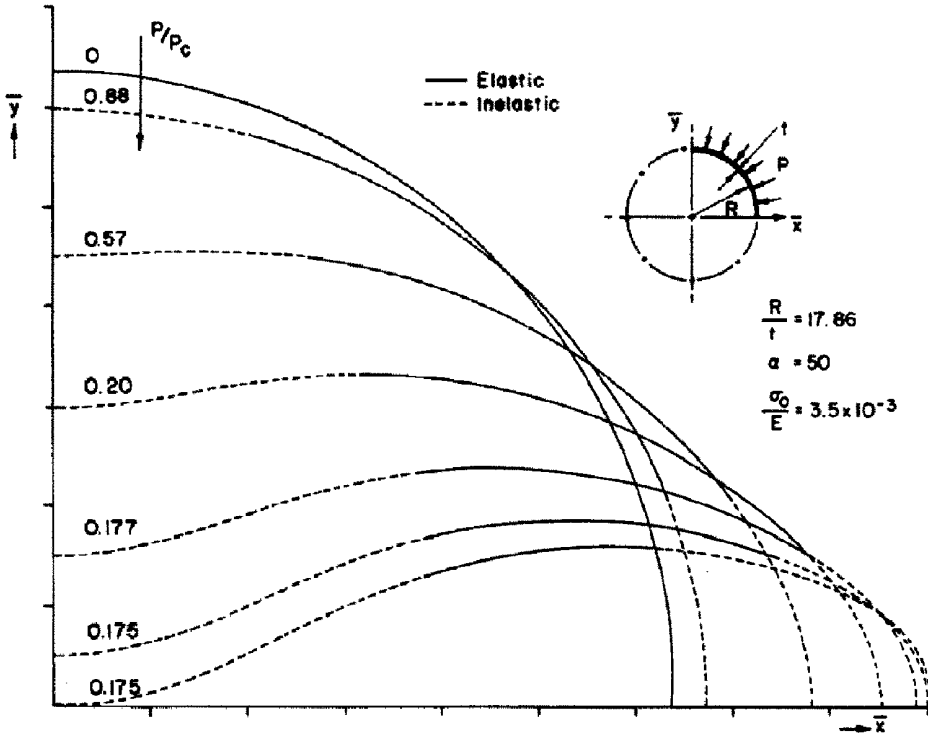


Fig. 7. Inelastic distribution on quadrant of collapsing ring.

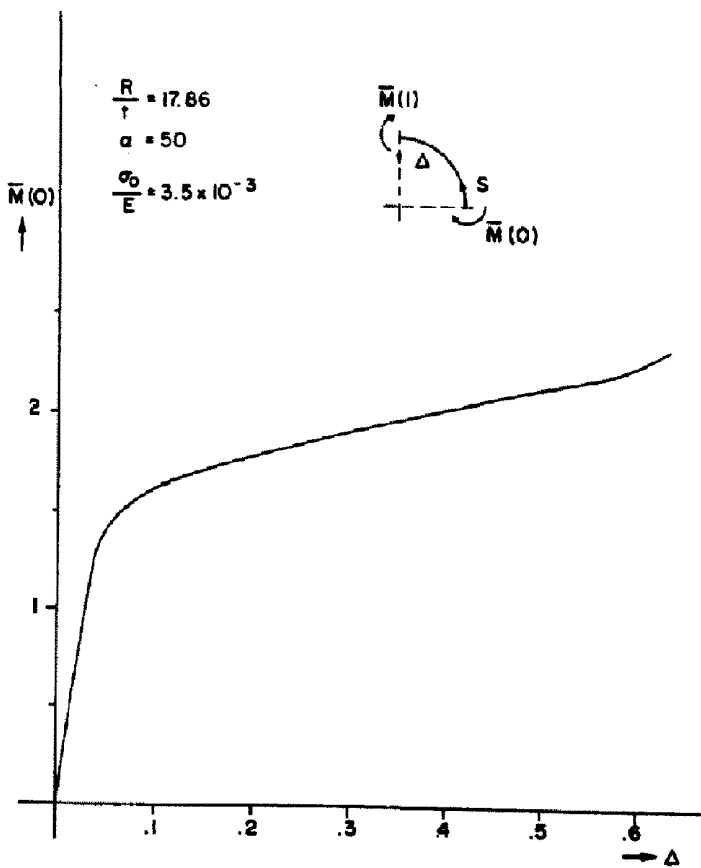


Fig. 8. Variation of moment at  $S = 0$  with displacement at  $S = 1$ .

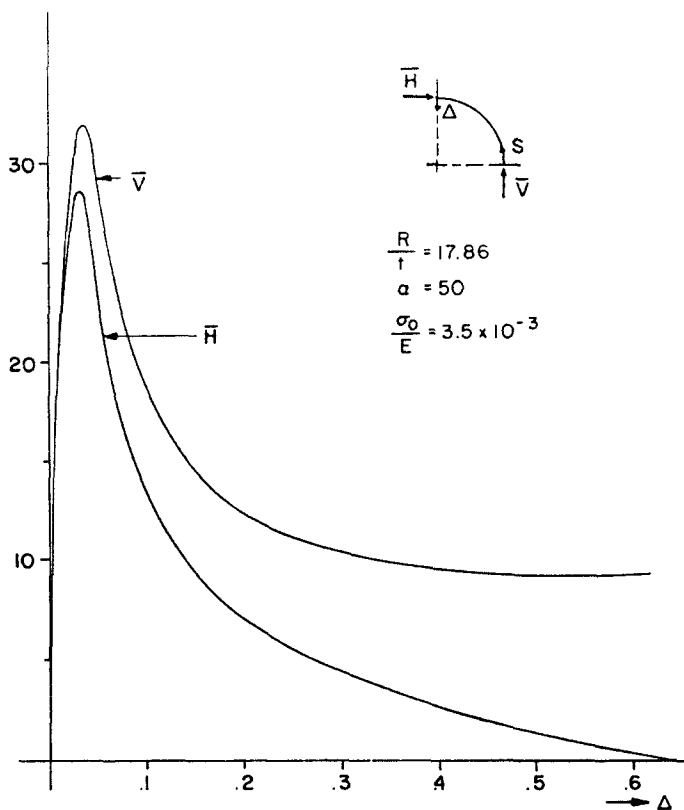


Fig. 9. Variation of end forces with displacement.

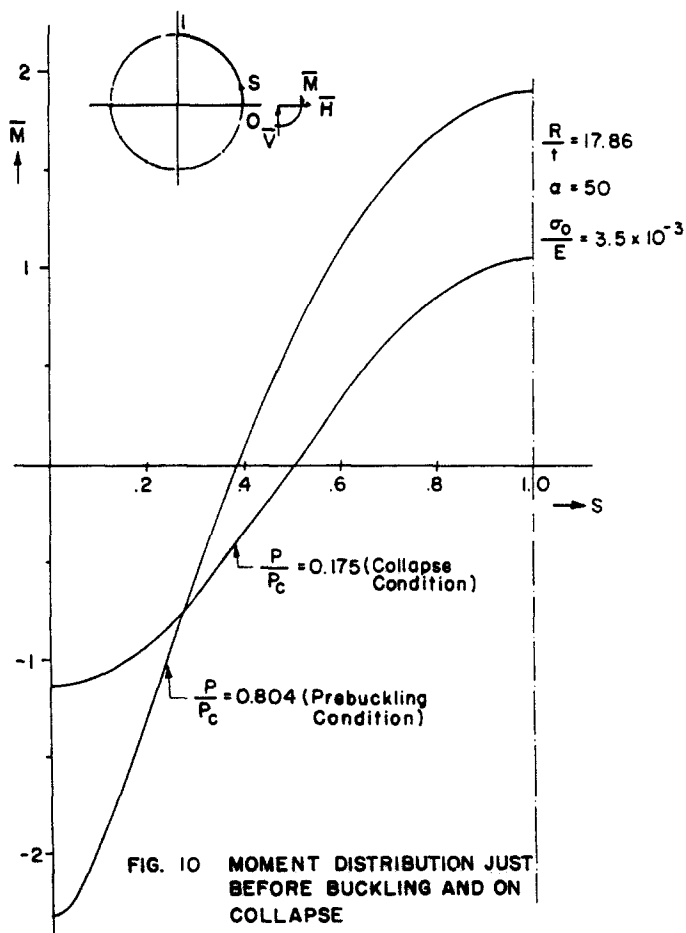


FIG. 10 MOMENT DISTRIBUTION JUST BEFORE BUCKLING AND ON COLLAPSE

Fig. 10. Moment distribution just before buckling and on collapse.

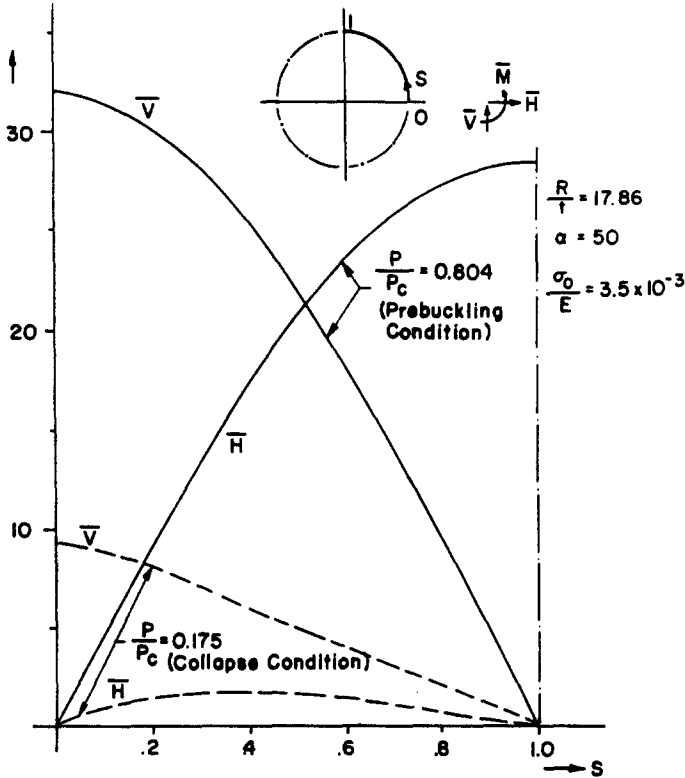


Fig. 11. Force distribution just before buckling and on collapse.

results are plotted for comparison on the same figure (Fig. 5). The difference between the elastic and inelastic cases is striking. Very soon after first yield occurs a distinct limit point is developed in the load displacement path. The response past this limit point becomes unstable. This limit load becomes effectively the buckling load of the ring. The value of the buckling load is imperfection sensitive as can be seen from the figure. The post-buckling behavior does not appear to be very sensitive to the value of the initial imperfection.

It is of interest to compare this behavior with that of the elastic case where, of course, the post-buckling behavior is stable. Obviously the response in that case is not imperfection sensitive. Looking at the collapse load in both cases it seems to be insensitive to the magnitude of the initial imperfection. As mentioned above, the limit load is reached very soon after first yield (limit load less than 2% higher than load at first yield). Clearly then the buckling load is sensitive to the yield stress of the material. Figure 12 shows a numerical example of the variation of the buckling load and generally the whole response with the yield stress ( $\sigma_0$ ).

Figure 13 shows how the post-buckling behavior is affected by the value of  $\alpha$ .  $\alpha$  represents a measure of the inelastic deviation from the elastic slope.  $\alpha = 1$  represents the purely elastic case and  $\alpha = 10^4$  represents what is practically an elastic perfectly plastic material behavior. The effect of strain hardening on the buckling load is insignificant; on the other hand, the post-buckling behavior which takes place in the elastoplastic regime is critically affected. For the case considered in Fig. 13  $\alpha = 1.5$  can cause the post-buckling path to become unstable. Although this represents only a specific case, it shows how sensitive the stability of the post-buckling path can be to deviations of the  $\sigma$ - $\epsilon$  behavior from the elastic modulus.

As mentioned in the introduction, Timoshenko[6] gives an expression for the small deflection elastic response of an inextensional ring with an initial imperfection under external pressure. He suggests that the collapse pressure of such a ring be taken to be equal to the pressure which causes first yield. From expression (23) of Ref. [6] this pressure in normalized form can be expressed as

$$\frac{P_x}{\sqrt{P_0 P_c}} = \frac{1}{2} \left\{ \left[ \frac{1}{\xi} + \left( 1 + 6 \frac{w_0}{t} \right) \xi \right] - \sqrt{\left[ \frac{1}{\xi} + \left( 1 + 6 \frac{w_0}{t} \right) \xi \right]^2 - 4} \right\},$$

where  $P_x$  = collapse pressure,  $P_0 = \sigma_0(t/R)$ ,  $P_c = E/4(t/R)^3$  and  $\xi = \sqrt{(P_c/P_0)}$ .

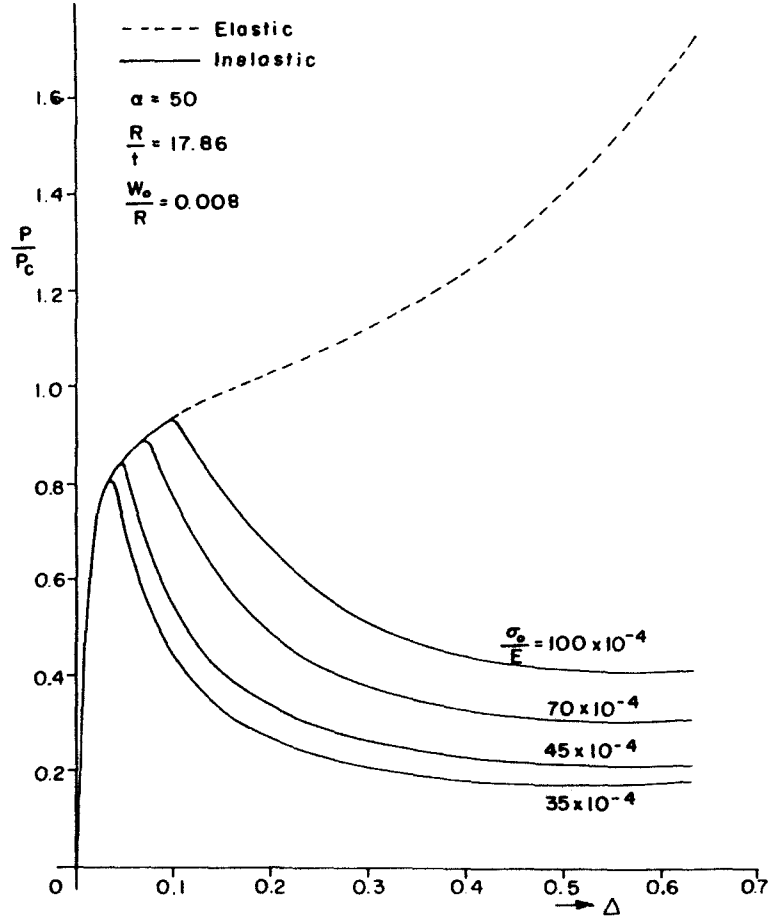


Fig. 12. Buckling sensitivity to yield stress.

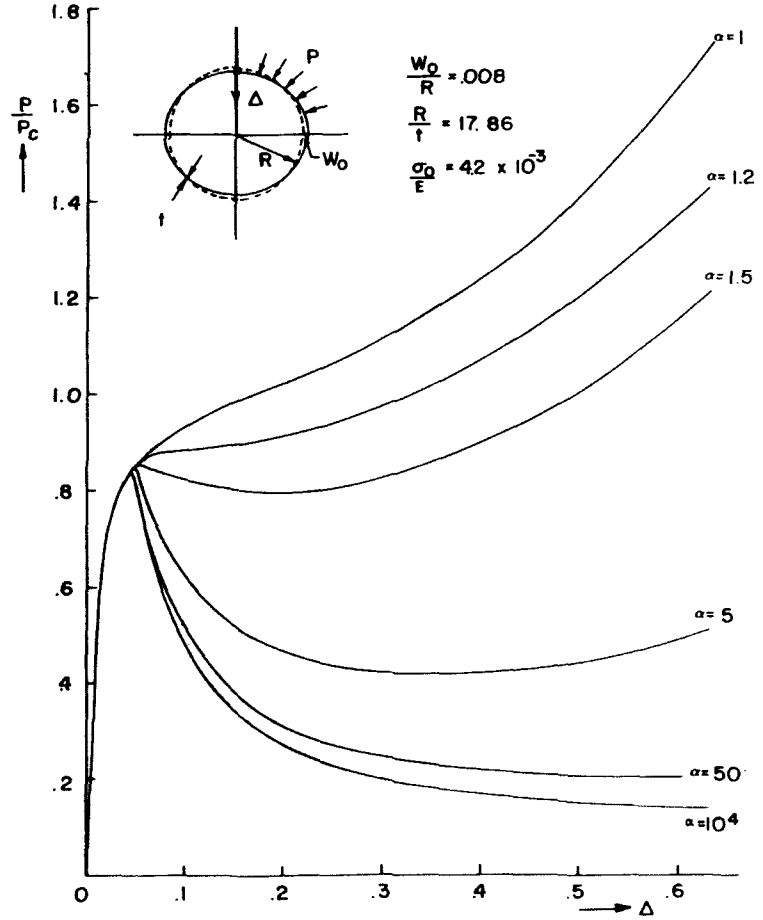


Fig. 13. Variation of postbuckling behavior with strain hardening parameter  $\alpha$ .

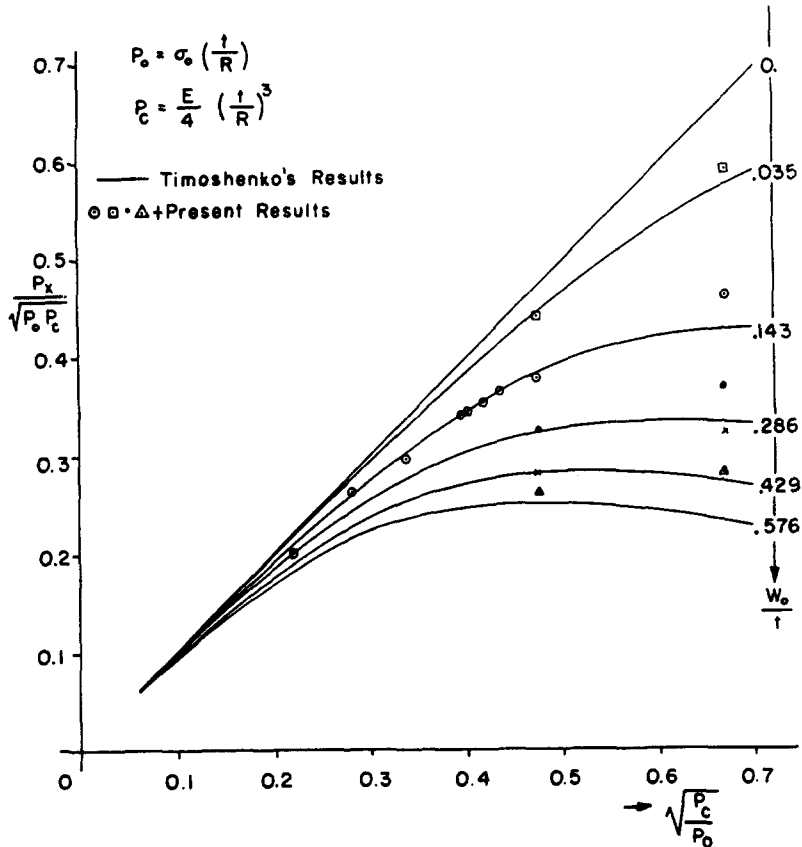


Fig. 14. Buckling results for different values of initial imperfection compared to Timoshenko's collapse criterion.

This expression is plotted in Fig. 14 for different values of the initial imperfection. On the same plot results from the current analysis are included for comparison. Buckling pressure is defined as the maximum pressure for which  $dp/d\Delta = 0$ . As is evident from Fig. 14, Timoshenko's criterion gives very good results for low values of  $\xi$  and small values of initial imperfection. For large  $\xi$  and larger  $w_0/t$  the criterion is conservative. It should be pointed out, however, that for large  $\xi$  the inextensibility assumption used by both Ref. [6] and the present analysis is not justified and corrections for membrane deformations become necessary.

*Acknowledgement*—The authors would like to thank Mr. P. Wong for helping with the computational part of the problem and Mrs. Maureen Matteson for typing the manuscript. The paper was prepared with the support of the U. S. Department of Energy Grant No. EX-76-G-03-1305. However, any opinions, findings, conclusions or recommendations expressed herein are those of the authors and do not necessarily reflect the views of DOE.

#### REFERENCES

1. G. F. Carrier, On the buckling of elastic rings. *J. Mathematics and Physics* 26, 94-103 (1947).
2. M. S. El Naschie, The initial postbuckling of an extensional ring under external pressure. *Int. J. Mech. Sci.* 17, 387-388 (1975).
3. J. G. Simmonds, Accurate nonlinear equations and a perturbation solution for the free vibration of a circular elastic ring. *J. Appl. Mech.* 46, 50-100 (March 1979).
4. L. W. Rehfield, Initial post buckling of circular rings under pressure loads. *J. AIAA* 10, 1358-1359 (Oct. 1972).
5. L. B. Sills and B. Budiansky, Post buckling ring analysis. Brief note. *J. Appl. Mech.* 45, 208-210 (March 1978).
6. S. Timoshenko, Working stresses for columns and thin-walled structures. *Trans. ASME, Appl. Mech. Div.* 1, 173-185 (1933).
7. A. C. Palmer, Buckle propagation in submarine pipelines. *Nature* 254 (5495), 46-48 (6 March 1975).
8. R. Mesloh, T. G. Johns and J. E. Sorenson, The propagating buckle. *BOSS* 76, *Proceedings* 1, 787-797 (1977).
9. S. Kyriakides and C. D. Babcock, On the dynamics and the arrest of the propagating buckle in offshore pipelines. *OTC* 3479, 1035-1045 (May 1979).
10. S. Kyriakides and C. D. Babcock, On the 'Slip-On' buckle arrestor for offshore pipelines. *J. Pressure Vessel Technology-Trans. ASME* 102, 188-193 (May 1980).
11. M. Lentini and V. Pereyra, An adaptive finite difference solver for nonlinear two-point boundary value problems with mild boundary layer. *SIAM, J. Numl. Anal.* 14, 91-111 (1977).
12. I. Tadjbakhsh and F. Odeh, Equilibrium states of elastic rings. *J. Math. Anal. and Application* 18, 59-74 (1974).
13. J. Arbocz, On the problem of limit point calculations. *GALCIT SM75-7* (1975).